RSC Advances

REVIEW

View Article Online
View Journal | View Issue



Cite this: *RSC Adv.*, 2021, **11**, 25354

# Green synthesis of carbon dots and their applications†

Shawninder Chahal,[a] Jun-Ray Macairan,[b] Nariman Yousefi,[c] Nathalie Tufenkji[ad] and Rafik Naccache[*bd]

Carbon dots (CDs) are nanoparticles with tunable physicochemical and optical properties. Their resistance to photobleaching and relatively low toxicity render them attractive alternatives to fluorescent dyes and heavy metal-based quantum dots in the fields of bioimaging, sensing, catalysis, solar cells, and light-emitting diodes, among others. Moreover, they have garnered considerable attention as they lend themselves to green synthesis methods. Increasingly, one-pot syntheses comprising exclusively of renewable raw materials or renewable refined compounds are gaining favor over traditional approaches that rely on harsh chemicals and energy intensive conditions. The field of green CD synthesis is developing rapidly; however, challenges persist in ensuring the consistency of their properties (*e.g.*, fluorescence quantum yield) relative to conventional preparation methods. This has mostly limited their use to sensing and bioimaging, leaving opportunities for development in optoelectronic applications. Herein, we discuss the most common green CD synthesis and purification methods reported in the literature and the renewable precursors used. The physical, chemical, and optical properties of the resulting green-synthesized CDs are critically reviewed, followed by a detailed description of their applications in sensing, bioimaging, biomedicine, inks, and catalysis. We conclude with an outlook on the future of green CD synthesis. Future research efforts should address the broad knowledge gap between CDs synthesized from renewable *versus* non-renewable precursors, focusing on discrepancies in their physical, chemical, and optical properties. The development of cost effective, safe, and sustainable green CDs with tunable properties will broaden their implementation in largely untapped applications, which include drug delivery, photovoltaics, catalysis, and more.

Received 17th June 2021
Accepted 12th July 2021

DOI: 10.1039/d1ra04718c

rsc.li/rsc-advances



## 1. Introduction

Carbon dots (CDs) are a class of fluorescent nanomaterials, typically less than ~10 nm in diameter, that can exhibit quantum dot-like behaviour. Since their initial discovery by Xu *et al.*,[1] CDs are now seen as potential alternatives to traditional fluorescent dyes owing to their versatile optical properties and resistance to photobleaching.[2] They also exhibit lower toxicity (both cyto- and chemical toxicity) in comparison to certain heavy metal-based quantum dots,[3] speaking to their potential for integration in biomedical applications.

Early CD syntheses employed top-down approaches whereby graphite was processed through multiple steps using harsh chemicals to transform it into the more usable graphite oxide[4] before it was broken down into nano-sized CDs.[5] Bottom-up synthesis methods, whereby smaller molecules polymerize and carbonize to form CDs, are increasingly attractive due to their ease of implementation and tunability. Recent efforts exploit renewable raw materials (*e.g.*, plants[6]), or renewable refined compounds (*e.g.*, citric acid, amino acids[7]) to synthesize CDs. The ability to tune and tailor the properties of CDs, prepared using sustainable materials and approaches, permits diverse application development in areas such as sensing,[8] bioimaging,[9] antibacterials,[10] fluorescent patterning inks,[11] and photocatalysis,[12] to name a few.

This review will first define the scope of green CD synthesis, followed by a discussion of the advantages and limitations of the various preparation methods, carbon sources, and purification protocols used. We will then discuss the size, chemical composition, and optical properties of green-synthesized CDs with an overview of their applications. We conclude with an outlook on the future of green CD synthesis and the knowledge gaps that remain to be addressed.

[a]*Department of Chemical Engineering, McGill University, 3610 University St, Montreal, Quebec H3A 0C5, Canada*

[b]*Department of Chemistry and Biochemistry, The Centre for NanoScience Research, Concordia University, 7141 Sherbrooke St. West, Montreal, Quebec H4B 1R6, Canada. E-mail: rafik.naccache@concordia.ca*

[c]*Department of Chemical Engineering, Ryerson University, 350 Victoria St, Toronto, Ontario M5B 2K3, Canada*

[d]*Quebec Centre for Advanced Materials, Canada*

† Electronic supplementary information (ESI) available. See DOI: 10.1039/d1ra04718c

# 2. Synthesis

## 2.1 What makes a synthesis green?

To answer this question, we will adopt aspects of the 12 Principles of Green Chemistry by Anastas and Warner,[13] specifically: (3) less hazardous chemical synthesis; (4) designing safer chemicals; (5) safer solvents and auxiliaries; (6) design for energy efficiency; (7) use of renewable feedstocks; and (12) inherently safer chemistry for accident prevention. These principles can be summarized as using non-toxic renewable precursors and solvents in a CD synthesis that is safe to perform. The synthesized CD itself should also be non-toxic and chemically stable. Although CD synthesis is generally an energy-intensive process, lower energy synthesis methods should be prioritized. Moreover, given the possibility of the formation of several side products and intermediates, one must consider their safety profile to ensure their proper disposal. These principles will guide us in the following subsections discussing previously reported green CD syntheses.

## 2.2 Green synthesis methods

Owing to its low cost and ease of implementation, hydrothermal synthesis is the most common green CD preparation method. This thermal-mediated approach requires pressurized autoclave vessels, reaction temperatures ranging from 120–240 °C, and reaction times of 3–12 h in a typical synthesis (Table 1). The definition of green synthesis stipulates using water (hydrothermal), or benign organic solvents (solvothermal) such as ethanol. The solvent can also be a renewable substance serving a dual purpose by acting as a carbon source in the synthesis (*e.g.*, walnut oil).[14] Solvent-free synthesis (*i.e.*, dry heating) is usually performed at temperatures as high as 300 °C under ambient pressure conditions (Table 1). Although simple to implement, these approaches require high temperatures and long reaction times. These reaction parameters can be readily optimized to maximize product yield and application-specific performance while minimizing energy requirements.

Microwave synthesis is advantageous as it enables direct heating of reaction mixtures, typically using ~800 W of microwave power for only a few minutes (Table 1). Despite these benefits, the entry point of microwave synthesis can be considerably more expensive as specialized equipment is needed. However, regular household microwaves have been used[15,16] with the trade-off of having less control over the synthesis parameters. Liu *et al.*[15] conducted a rapid, low-energy microwave synthesis at 800 W for 3 min; this rapid reaction time (60–240× faster than hydrothermal synthesis) highlights the increased heating efficiency of microwaves. Unlike hydrothermal synthesis that relies on conductive heat transfer, microwaves allow for direct and selective heating *via* resonance with the vibrational frequencies of molecules. Therefore, a microwave reaction is often complete before an appreciable change in temperature of an equivalent hydrothermal synthesis is attained.

## 2.3 Carbon source

Diverse plant types are used as renewable carbon feedstocks for green CD synthesis (Fig. 1a). The most commonly used parts of the plant are the leaves,[6] flowers,[32,33] or roots.[34] Other forms of plant biomass include shells,[30] kernels,[35] bark,[12] stalk,[19] and

Table 1 Processing parameters and properties of CDs synthesized by green methods[a]

| Carbon source | Method | Conditions | Size [nm] | N : C | O : C | Excitation [nm] | Emission [nm] | QY | Ref. |
|---|---|---|---|---|---|---|---|---|---|
| *Eleocharis dulcis* | Hydrothermal | 120 °C, 5 h | 3.0 | 0.05 | 0.33 | 380 | 458 | 11% | 17 |
| *Azadirachta indica* | Hydrothermal | 150 °C, 4 h | 3.2 | 0.09 | 0.12 | 340 | 467 | 27% | 18 |
| Maize | Hydrothermal | 160 °C, 10 h | 5.2 | 0.02 | 0.35 | 420 | 500 | 8% | 19 |
| Rose-heart radish | Hydrothermal | 180 °C, 3 h | 3.6 | 0.13 | 0.43 | 330 | 420 | 14% | 20 |
| *Ocimum sanctum* | Hydrothermal | 180 °C, 4 h | 2.4 | 0.18 | 0.35 | 450 | 500 | 9% | 8 |
| Scallion | Hydrothermal | 180 °C, 12 h | 3.5 | 0.12 | 0.27 | 320 | 418 | 3% | 21 |
| Strawberry | Hydrothermal | 180 °C, 12 h | 5.2 | 0.10 | 0.35 | 344 | 427 | 6% | 22 |
| Pomelo | Hydrothermal | 200 °C, 3 h | 2.9 | 0.06 | 0.35 | 365 | 444 | 7% | 23 |
| Willow | Hydrothermal | 200 °C, 3 h | 1.6 | 0.43 | 0.39 | 360 | 444 | 6% | 12 |
| Tulsi | Hydrothermal | 200 °C, 4 h | 5.0 | 0.10 | 0.89 | 360 | 435 | 3% | 11 |
| Citric acid, glutathione | Hydrothermal | 200 °C, 4 h | 6.1 | 0.20 | 0.26 | 340 | 432 | 75% | 24 |
| Citric acid, L-phenylalanine | Hydrothermal | 200 °C, 8 h | 11.9 | 0.14 | 0.36 | 350 | 413 | 65% | 7 |
| Citric acid, L-arginine | Hydrothermal | 200 °C, 8 h | 2.7 | 0.11 | 0.17 | 350 | 440 | 39% | 25 |
| Ginkgo | Hydrothermal | 200 °C, 10 h | 3.0 | 0.06 | 0.35 | 350 | 436 | 23% | 6 |
| *Tamarindus indica* | Hydrothermal | 210 °C, 5 h | 3.4 | 0.28 | 0.68 | 320 | 417 | 47% | 26 |
| *Allium fistulosum* | Hydrothermal | 220 °C, 3 h | 4.2 | 0.37 | 0.38 | 412 | 503 | 10% | 27 |
| *Abelmoschus manihot* | Hydrothermal | 220 °C, 4 h | 9.0 | 0.25 | 0.07 | 330 | 410 | 31% | 9 |
| *Osmanthus fragrans* | Hydrothermal | 240 °C, 5 h | 2.2 | 0.04 | 0.38 | 340 | 411 | 19% | 28 |
| Walnut | Solvothermal | 220 °C, 24 h | 12.3 | 0.05 | 1.12 | 360 | 430 | 15% | 14 |
| Watermelon | Dry heating | 220 °C, 2 h | 2.0 | 0.02 | 0.31 | 470 | 537 | 7% | 29 |
| Peanut | Dry heating | 250 °C, 2 h | 1.6 | 0.04 | 0.49 | 320 | 440 | 10% | 30 |
| Bamboo | Dry heating | 300 °C, 3 h | 11.0 | 0.06 | 1.00 | 313 | 419 | 5% | 31 |
| Glycine, urea | Microwave | 800 W, 3 min | 3.2 | 0.40 | 0.42 | 320 | 380 | 13% | 15 |
| Lotus | Microwave | 800 W, 6 min | 9.4 | 0.09 | 0.53 | 360 | 435 | 19% | 16 |

[a] QY = quantum yield.

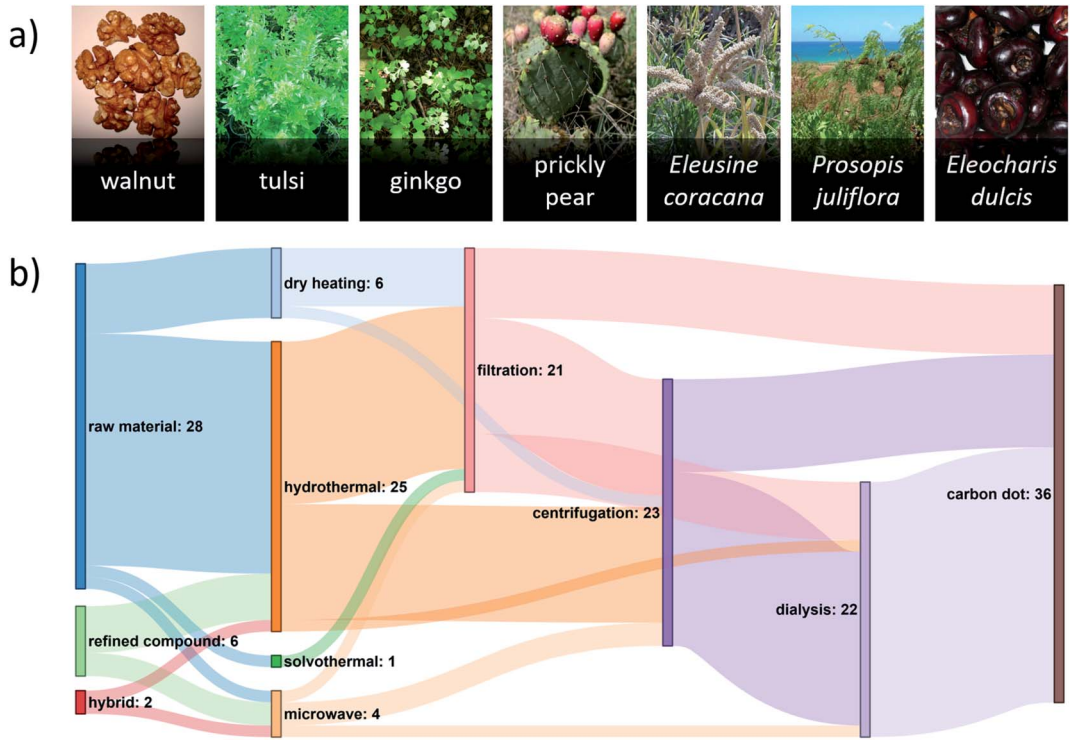


Fig. 1 (a) A diverse set of locally sourced renewable precursors can be used for the green synthesis of CDs. A reference list of these images can be found in Table S1 of the ESI.† (b) Sankey diagram showing the number of green-synthesized CD publications reporting various pathways from carbon source to CD. For this diagram, it is assumed that the purification steps followed the order: (1) filtration, (2) centrifugation, (3) dialysis, although this was not always the case, and this assumption was made for illustrative purposes only. A hybrid precursor indicates that both a renewable raw material and renewable refined compound were used. The most common synthesis route uses a renewable raw material in a hydrothermal synthesis followed by one or more purification steps. A reference list can be found in Table S2 of the ESI.†

peels.[23,29] Such feedstocks require preprocessing to reduce particle size and remove excess water. Drying the feedstock under direct sunlight[35,36] reduces energy requirements relative to conventional dehydration routes. The use of fruit juice[22] can be convenient as it provides a "ready-to-use" solution for hydrothermal synthesis, avoiding the need to redisperse dried plant matter in water. However, this benefit comes at the cost of the carbon diversity found in the dry feedstock.

Renewable refined compounds (*i.e.*, compounds that can be synthesized through naturally occurring bioprocesses) have also been used in CD synthesis. For instance, Zhang *et al.* performed a hydrothermal CD synthesis from citric acid and the amino acid L-arginine,[25] whereas Liu *et al.* used urea and the amino acid glycine in a microwave synthesis of CDs.[15] While renewable refined compounds may not be as strictly green as the direct use of renewable raw materials, their synthesis can remain sustainable. For instance, Lotfy *et al.* prepared citric acid with an 88% yield from the fungus *Aspergillus niger* by using beet molasses, corn steep liquor, and salts as a feedstock.[37] Citric acid is also abundant in Nature, most notably in *Citrus* fruits, where the dry fruit mass consists of up to 8% citric acid.[38] Moreover, hybrid green syntheses have also been performed through the mixture of renewable raw materials and renewable refined compounds, such as the use of celery leaves and L-glutathione in a hydrothermal CD synthesis.[39]

### 2.4 Purification

The purification of the post-synthesis CD reaction mixture is a crucial step in the production of carbon dots as it contains a myriad of side-products and unreacted precursors with varying solubilities and sizes. Indeed, the removal of side-products that possess different size and dispersibility profiles relative to the CDs, would suggest that a multi-step purification process is typically required. Extensive purification procedures are carried out with the aim of obtaining CDs with uniform physical and optical properties.[40] Poor purification can impact CDs' potential use in certain applications. For instance, Essner *et al.* demonstrated that inadequate purification steps can greatly impact the sensing performance of CDs due to the presence of fluorescent impurities.[41]

Carbon dot purification typically relies on a combination of multiple methods. Large insoluble matter is typically removed through centrifugation and/or filtration.[28] In the former, insoluble impurities will be found at the bottom of the tube after centrifugation – thus enabling easy separation from the supernatant, which typically contains the CDs. In the latter, impurities larger than the pore size of the filter will be excluded from the filtrate. Dialysis is another purification method which is typically performed over a 24–72 h period to remove any remaining small soluble impurities.[6,16] These three methods are evenly implemented (Fig. 1b) (although in varying order) in green CD syntheses with the goal of minimizing the presence of any impurities.

# 3. Properties

## 3.1 Size

Typically, green-synthesized CDs can be prepared with a diameter of 2–12 nm,[14,30] as measured using transmission electron microscopy (TEM). A size distribution of green-synthesized CDs found in the literature is shown in Fig. 2d and reveals that the majority of these CDs fall within the lower end of this size range. Tailoring the size of these semiconductor-like dots can enable them to confine photons *via* modulation of their bandgap.[42] Fig. 2a shows a typical high-resolution TEM image of a CD (synthesized from black pepper) with crystallographic information obtained from its lattice order and spacing.[43] Conversely, amorphous CDs lack a periodic crystal lattice,[25] cannot diffract electrons,[44] and may show an X-ray diffraction pattern with a broad reflection (amorphous halo) that has a peak in the $2\theta = 23.4–24.6°$ region.[45]

A challenging aspect of TEM imaging of CDs, especially those that are amorphous, is that their composition closely resembles that of the formvar-coated TEM grids they are typically imaged on. Moreover, deposition on the TEM grid must be done with care to minimize aggregation that could lead to sizing artefacts.[47] Atomic force microscopy (AFM) can also be used for size measurements, providing length, width, and height information of the CDs.[7] This method avoids the contrast issues that may arise with electron microscopy of carbon nanomaterials. Ideally, both AFM and TEM should be used in conjunction to obtain both size and topographic information. In what concerns biological applications of CDs, dynamic light scattering measurements are critical as they provide a hydrodynamic radius.[46] This measurement is directly related to the diffusivity of the CDs in biological environments. Independent of size, CDs can form in quasi-spherical morphologies, including hollow CDs (Fig. 2b) with an architecture that facilitates their use as a drug delivery agent.[46]

## 3.2 Optical properties

A characteristic property of CDs is their ability to fluoresce under UV irradiation. However, the CD fluorescence mechanism remains a topic of debate and is suspected to vary according to the synthesis parameters. The CD surface properties (*e.g.*, degree of oxidation, decoration with functional groups), size-dependant quantum confinement effect, and the incorporation of fluorescent molecules at the CD core or surface can all impact the mechanism.[42] Fig. 2f summarizes the excitation/emission wavelength relationship for green-

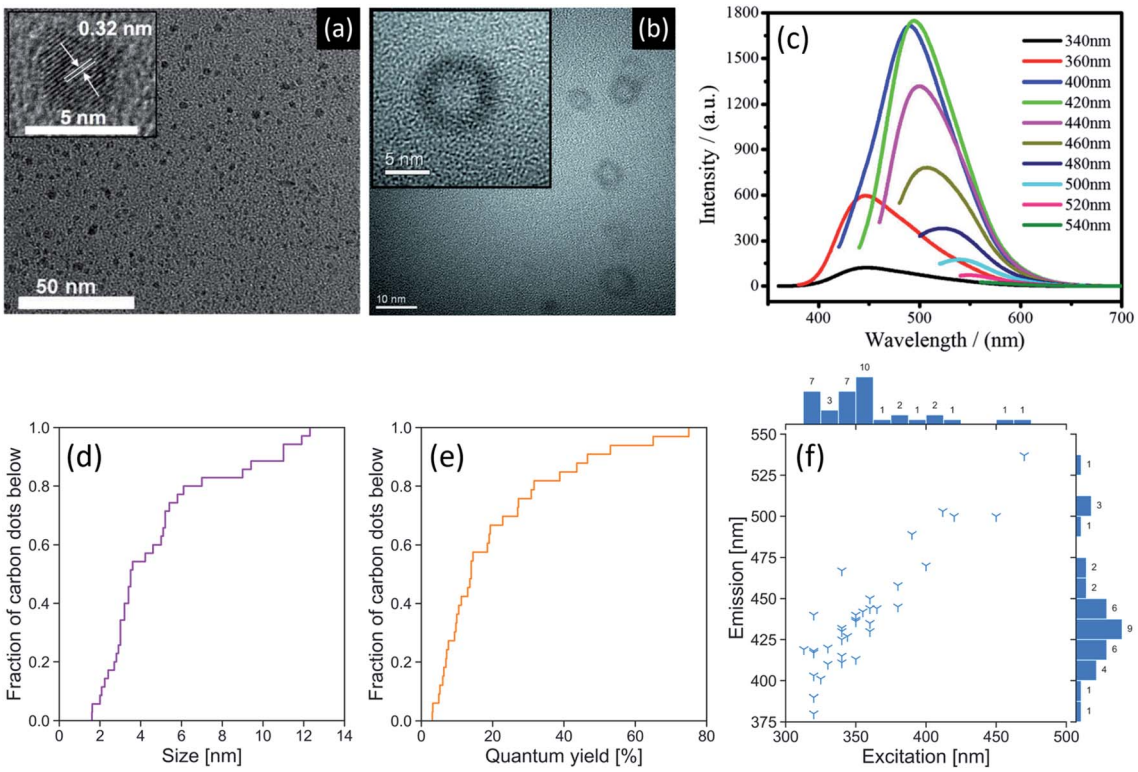


Fig. 2 (a) HR-TEM images of CDs synthesized from black pepper (inset: lattice spacing). Adapted from Open Access ref. 43. Copyright 2018 Vasimalai *et al.*; licensee Beilstein-Institut. (b) HR-TEM images of hollow CDs synthesized from bovine serum albumin. The hollow design allows for this CD to be used in drug delivery applications. Adapted with permission from ref. 46. Copyright 2013 Elsevier Ltd. (c) Fluorescence spectra of a CD synthesized from maize at different excitation wavelengths. These CDs displayed green colour at their peak fluorescence emission. Adapted with permission from ref. 19. Copyright 2017 Springer Science Business Media Dordrecht. Empirical cumulative distribution function plots of (d) CD size as measured by TEM and (e) fluorescence quantum yield. (f) Peak excitation and emission wavelengths of green-synthesized CDs. Counts are shown next to their respective bins and indicate the number of publications reporting CDs with properties in that bin's range. Peak emission and excitation generally move in the same direction. A reference list can be found in Table S2 of the ESI.†

synthesized CDs extracted from 36 studies. Half of these CDs (1st–3rd quartile) have peak excitations between 330–360 nm. The CDs in this peak excitation range have corresponding emissions ranging from 410–467 nm. Fig. 2c shows the fluorescence spectra of a CD with a green colour fluorescence emission at 500 nm upon excitation at 420 nm,[19] which is higher than the typical range. We note a general trend of increasing peak emission wavelength with increasing peak excitation wavelength.

The ability to tailor the peak emission wavelength as a function of the excitation wavelength is a desirable feature in bioimaging as it can minimize autofluorescence of cells and tissues by selecting an excitation wavelength that generates fluorescence of the CD, but not of the sample to be imaged. For instance, Zhou *et al.* synthesized CDs from watermelon peel with a maximum fluorescence intensity at an excitation/emission wavelength of 470/535 nm corresponding to a blue/green excitation/emission.[29] This can be useful for imaging biological samples with a high degree of autofluorescence under UV excitation, but with minimal autofluorescence under blue excitation.

Carbon dot fluorescence typically involves high-energy photon absorbance and lower energy emission; however, some CDs can undergo multiphoton excitation whereby they can upconvert longer wavelengths of light to emit higher energy photons. This phenomenon is desirable in applications such as bioimaging by enabling the use of lower energy excitation wavelengths that can reduce the risk of cell damage while simultaneously enhancing penetration depth.[48] Liang *et al.* synthesized CDs from gelatin which, in addition to exhibiting conventional fluorescence ($\lambda_{ex}$ = 350, $\lambda_{em}$ = 430 nm), also underwent photon upconversion following 750 nm excitation with an emission at 450 nm.[49]

The fluorescence quantum yield (QY) of a CD, *i.e.*, the ratio of the number of photons emitted to the number of photons absorbed,[50] is a useful metric as it is theoretically independent of concentration and instrumentation, allowing for direct comparison of QYs across the literature. Green-synthesized CDs reportedly have QYs ranging from 3–75%, with a median QY of 14% (Fig. 2e). We have thus far praised the various benefits of using green synthesis methods to produce CDs. Yet, achieving high QYs using green synthesis methods lags relative to conventional preparation approaches. For instance, one of the highest QYs achieved by a CD synthesized from renewable raw materials is 47% using *Tamarindus indica* leaves.[26] To our knowledge, one of the highest QYs achieved by a CD synthesized from renewable refined compounds is 75% using citric acid and glutathione.[24] However, a QY of 99% has been achieved using citric acid and the non-renewable tris(hydroxymethyl)aminomethane.[51] The observed discrepancies in QY measurements can arise from two principal factors. Firstly, we must consider the heterogeneity of plant-based carbon sources that often comprise a mixture of carbohydrates, lipids, proteins, and nucleic acids. With more efficient extraction methods, it would

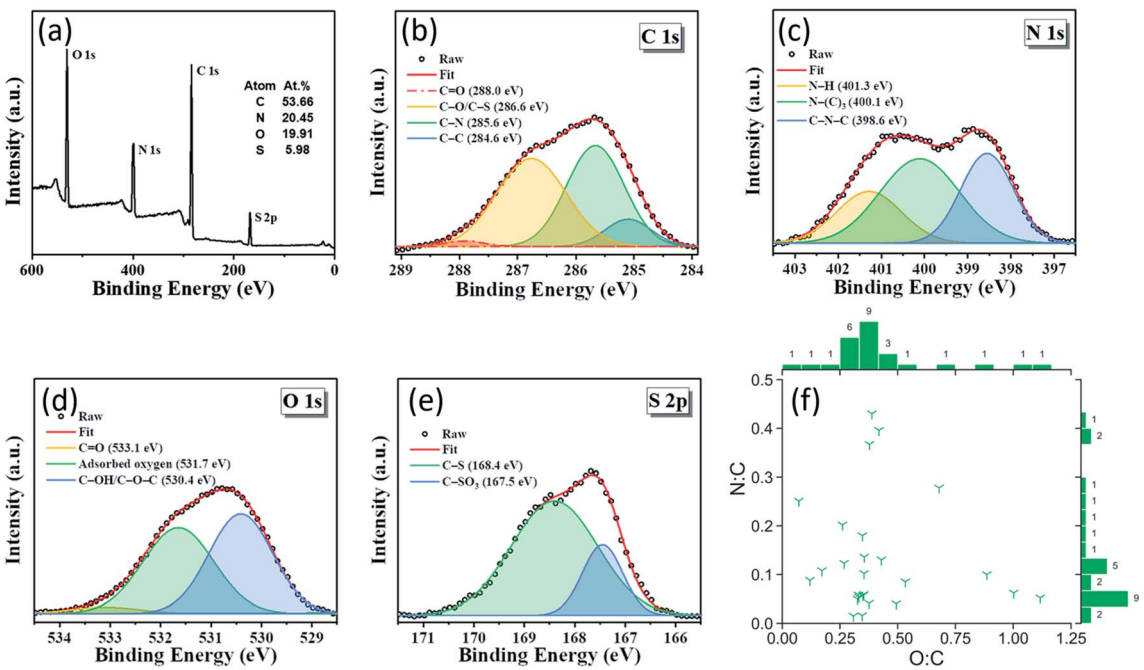


Fig. 3 (a–e) XPS spectra of CDs showing nitrogen and sulfur doping. The use of *Allium fistulosum* in synthesis gave access to an abundant and diverse set of biomolecules contained within the plant resulting in an elementally diverse CD with a high sulfur content. Adapted from RSC ref. 27. Copyright 2019 the Centre National de la Recherche Scientifique (CNRS) and The Royal Society of Chemistry. (f) Plot showing the diverse range of the O : C and N : C ratios of green-synthesized CDs reported in the literature. Counts are shown next to their respective bins and indicate the number of publications reporting CDs with properties in that bin's range. N : C and O : C are atomic ratios. XPS data from publications were assumed to be in atomic percent whereas elemental data from other types of instrumentation were either explicitly stated as atomic ratios or converted from their mass ratios. A reference list can be found in Table S2 of the ESI.†

be possible to isolate the desired starting materials *in lieu* of using the whole plant. Secondly, the absolute QY values are intimately tied to the purification protocols that serve to remove unreacted starting materials and fluorophores.[40] Indeed, purification of CDs is a step in the synthesis process that has not been standardized.

### 3.3 Chemical composition

Doping CDs with a heteroatom such as nitrogen is common practice since it is known to enhance QY by modifying the electronic properties and surface chemistry of the CDs.[52] Moreover, while the presence of oxygen in green-synthesized CDs is common due to the abundance of oxygen in renewable raw materials and also many organic compounds, they can also impact the QY by affecting the degree of oxidation of the CDs.[7] Renewable raw materials are a source of heteroatoms such as nitrogen, sulfur, and phosphorus. X-ray photoelectron spectroscopy (XPS) is commonly used to measure the CD elemental composition on an atomic basis. In the green CD literature, CDs have an oxygen-to-carbon (O : C) ratio of 0.07–1.12, and a nitrogen-to-carbon (N : C) ratio of 0.02–0.43 (Fig. 3f). CDs synthesized from *Allium fistulosum* exhibit a sulfur-to-carbon (S : C) ratio of 0.11 (Figure 3a),[27] while those prepared from *Eleocharis dulcis* contained traces of phosphorus resulting in a phosphorus-to-carbon (P : C) ratio of 0.004.[17] The elemental diversity of renewable raw materials can be advantageous when synthesizing hetero-doped CDs, but complicate our ability to tune the chemical composition of the CDs. In such cases, renewable refined compounds should be used. Fig. 3b–e shows a typical XPS spectra for a CD's different elements.

Despite being synthesized from a wide variety of precursors, half of the CDs in Fig. 3f have an O : C ratio in the narrow 0.31–0.39 region. Cellulose is a major plant component, but has an O : C ratio of 0.83, well above the range indicated. Thermal reduction has been observed in complex compounds similar to CDs. For example, Chen *et al.* were able to thermally reduce graphene oxide with an O : C ratio of 0.48 to partially reduced graphene oxide with an O : C ratio of 0.18, as measured by XPS, using microwave irradiation.[53] Therefore, it is possible that the cellulose in plants, along with other biomolecules, is thermally reduced to a similar extent in reported studies, leading to similar O : C ratios in the resulting CDs. Another possible explanation for this convergence to a common O : C ratio could be that the CD is more likely to form a chemically stable structure in this region.

## 4. Applications

### 4.1 Chemical sensing

There is growing interest in CDs as inexpensive and sensitive chemical nanosensors (Table 2). Chemical sensing is typically

Table 2 Summary of the sensing properties of green-synthesized CDs[a]

| Analyte | Method of detection | Limit of detection | Linear range | Ref. |
|---|---|---|---|---|
| $As^{3+}$ | FQ | 2.3 nM | 2–12 nM | 54 |
| $ClO^-$ | FQ | 16 nM | 10–90 μM | 54 |
| $Cr^{6+}$ | FQ | 4.5 ppb | 1.6–50 μM | 11 |
| $Cu^{2+}$ | FQ | 10 nM | 0–100 μM | 55 |
| $Fe^{2+}$ | FQ | 180 nM | 0–18 μM | 19 |
| $Fe^{3+}$ | FQ | 5 nM | 0.01–50 μM | 28 |
| $H_2O_2$ | AI | 35 μM | 100–500 μM | 18 |
| $Hg^{2+}$ | FQ | 0.23 nM | 0.5–10 nM | 23 |
| 2,4,6-Trinitrophenol | FQ | 5 nM | 0.025–40 μM | 9 |
| Adenosine triphosphate | FI | 5 nM | 0.01–450 μM | 33 |
| Ascorbic acid | AI | 1.773 μM | 5–40 μM | 18 |
| Dimercaptosuccinic acid | FI | 1.4 ng $mL^{-1}$ | 2.5–22.5 ng $mL^{-1}$ | 56 |
| Chlortetracycline | FQ | 0.078 μg $mL^{-1}$ | 0.85–20.38 μg $mL^{-1}$ | 25 |
| Cysteamine | FQ | 75.6 nM | 10–210 μM | 57 |
| Doxorubicin | FQ | 0.4 ng $mL^{-1}$ | 1–400 ng $mL^{-1}$ | 58 |
| Glutathione | FI | 1.7 μM | 0–20 μM | 26 |
| Glyphosate | FI | 12 ng $mL^{-1}$ | 0.025–2.5 μg $mL^{-1}$ | 59 |
| Imipramine | FQ | 0.6 ng $mL^{-1}$ | 1.0–200.0 ng $mL^{-1}$ | 34 |
| Methotrexate | FQ | 7 nM | 0.02–18.0 μM | 10 |
| Morin | FQ | 0.12 μM | 0.4–60 μM | 15 |
| Penicillamine | FQ | 0.02 μg $mL^{-1}$ | 0.05–13.0 μg $mL^{-1}$ | 60 |
| Prilocaine | FQ | 1.8 nM | 2.3–400 nM | 61 |
| Pyridine | FI | 210 nM | 0.5–4.1 μM | 62 |
| Salazosulfapyridine | FQ | 40 nM | 0.1–80 μM | 6 |
| Sulfasalazine | FQ | 0.032 μg $mL^{-1}$ | 0.34–6.76 μg $mL^{-1}$ | 25 |
| Trifluralin | FQ | 0.5 nM | 0.050–200 μM | 63 |
| Zoledronic acid | FI | 40 nM | 0.1–10 μM | 35 |

[a] FQ = fluorescence quenching, FI = fluorescence increase, AI = absorbance increase.

performed by monitoring changes in CD fluorescence or absorbance in the presence of a target analyte. The presence of heteroatoms can potentially improve sensing performance and be tailored to interact with specific analytes. For instance, N/P-doped CDs synthesized from *Eleocharis dulcis* juice exhibit high selectivity towards $Fe^{3+}$ relative to other metals.[17] The high affinity of these CDs towards $Fe^{3+}$ stems from the presence of nitrogen and oxygen groups that allow for rapid chelation.[17] A static fluorescence quenching mechanism is usually operative, indicating the formation of a non-radiative complex between the CD and the metal ion.[7] Amin *et al.* synthesized CDs from date kernels, which were used to detect zoledronic acid – an anticancer agent.[35] Initially, $Fe^{3+}$ quenches the fluorescence of the CDs *via* the formation of a complex.[35] Subsequently, $Fe^{3+}$ is chelated from the CD surface by zoledronic acid thereby restoring CD fluorescence with a 40 nM detection limit.[35] This CD sensor was successfully used in human serum, which increases its utility for routine zoledronic acid monitoring.[35] Similarly, Ramezani *et al.* used quince to synthesize CDs which, when coupled with $MnO_4^-$, can detect $As^{3+}$.[64] The CDs make use of the fact that $MnO_4^-$ oxidizes both CDs and $As^{3+}$, therefore the presence of $As^{3+}$ in an $MnO_4^-$ solution will result in fewer CDs being oxidized, and in turn less fluorescence quenching.[64] Future research in green CD sensing may consider these unique approaches to sensing analytes as opposed to the traditional methods which rely on direct CD-analyte interactions. Doing so, along with gaining a deeper understanding of the role of the physical, chemical, and optical properties of the CDs, can help improve the detection limits of future green-synthesized CDs. Note that in Table 2, a fluorescence increase (FI) may originate from the recovery of fluorescence from a previously quenched CD or from the actual increase of fluorescence intensity of the original CD.

### 4.2 Bioimaging

Bioimaging is one of the most studied applications of CDs due to their generally low cytotoxicity[3] and resistance to photobleaching.[2] CDs have been used as bioimaging probes both *in vitro* (*e.g.*, in A549 (ref. 28) and HeLa cells[9]) and *in vivo* (*e.g.*, zebrafish[65]). CDs synthesized from watermelon peels were used to image HeLa cells, demonstrating that CDs can be good candidates for bioimaging due to their stability in aqueous solutions, small size, and strong fluorescence.[29] Some CDs exhibit excitation-dependent fluorescence allowing for their use in multicolour fluorescence imaging. This feature can be useful when imaging cells, tissues, or organisms which exhibit auto-fluorescence by allowing the user to easily switch between fluorescence wavelengths while using a single type of CD. In doing so, the user may quickly identify a wavelength that does not interfere with the natural fluorescence of their sample. For example, CDs derived from peanut shells were used to image HepG2 cells using excitation wavelengths of 405, 488, and 514 nm which resulted in blue, green, and red emission, respectively.[30] Similarly, CDs synthesized from *Allium fistulosum* were used to image MCF-7 and K562 cells using excitation wavelengths of 405, 488, and 561 nm which resulted in blue, green, and red emission, respectively.[27] CD surfaces can also be passivated with functional groups and heteroatoms that can impact their cytotoxicity and potential localization in cells. Dehvari *et al.* synthesized CDs from crab shells and functionalized the CDs with folic acid for targeted imaging of HeLa cells that possess significantly more folate-receptors than healthy cells.[66] These CDs showed enhanced uptake in cancer cells relative to their non-cancerous counterpart.[66]

CDs synthesized using green approaches have also been used for *in vivo* imaging. Zebrafish embryos exhibited a ~93% survival rate (at 96 hours since fertilization) after 94 h of exposure to $\leq$ 200 μg $mL^{-1}$ CDs synthesized from gynostemma, compared to a ~97% survival rate in the control, showing that these CDs can be safely used for bioimaging (Fig. 4). However, the survival rate decreased to ~88% when the CD concentration increased to 400 μg $mL^{-1}$.[65] These CDs also showed antioxidant properties, effectively reducing the oxidative stress in the zebrafish, which may be partially responsible for their low

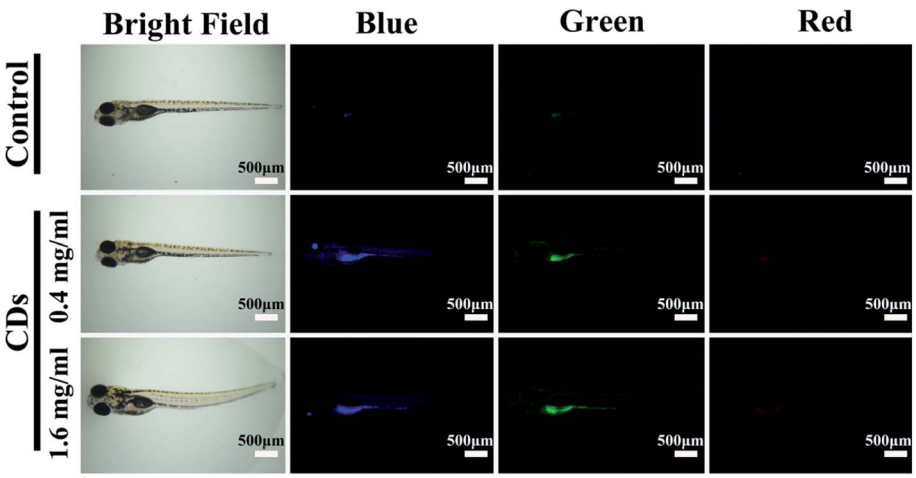


Fig. 4 Zebrafish imaging using CDs synthesized from gynostemma. It is demonstrated that the probes localize in the digestive system. The CDs exhibit blue, green, or red fluorescence depending on the excitation source used. Reprinted with permission from ref. 65. Copyright 2019 American Chemical Society.

toxicity.[65] Altogether, their study shows the importance of finding an optimal CD concentration which provides adequate imaging power while also minimizing toxicity to the organism or cells to be imaged.

Most CD bioimaging probes localize in the cytoplasm and accumulate just outside the nucleus,[43,57] while some have been reported to also enter the nucleus itself.[8] While these features are sufficient for general purpose bioimaging of cells, targeting specific organelles may also be of interest. The green synthesis of selectively localizing CDs is one area which merits further research to expand CD bioimaging applicability.

### 4.3 Biomedicine

CDs show promise in biomedical applications, in part due to the myriad of functional groups that decorate their surface, which allows for active targeting. For instance, Wang *et al.* used bovine serum albumin to develop a 6.8 nm hollow CD (HCD) loaded with doxorubicin.[46] After 90 minutes of incubation with the doxorubicin–HCD complex, red fluorescence stemming from the drug was observed in the nucleus of A549 cells.[46] The authors proposed a mechanism whereby the doxorubicin–HCD complex enters the cell through endocytosis and upon entering the lower pH lysosome, the complex releases the doxorubicin which then enters the nucleus.[46] Shao *et al.* have also synthesized CDs from mulberry leaves which were subsequently loaded with the anti-cancer drug lycorine.[67] Their lycorine-CD platform showed enhanced cell death in the cancerous HepG2 cell line when compared to lycorine alone.[67] CDs have also been used in antimicrobial applications. For instance, CDs synthesized from henna leaves were found to be much more effective antimicrobial agents than the bulk henna leaves against both Gram-positive *Staphylococcus aureus* and Gram-negative *Escherichia coli*.[10]

### 4.4 Ink

Inexpensive fluorescent inks for anti-counterfeiting applications (*e.g.*, invisible security inks) have been developed using green-synthesized CDs. For instance, CDs synthesized from oriental plane leaves were used as fluorescent inks to print patterns that were invisible under daylight and became visible under UV light (Fig. 5).[68] Similarly, Wang *et al.* have synthesized CDs from milk which were used as fluorescent inks.[69] They were able to refill regular commercial inkjet cartridges with their CDs which were then used to produce fluorescent patterns on commercial paper.[69] The printed patterns exhibited green and red fluorescence under 455 and 523 nm excitation, respectively.[69] In another green synthesis, Qu *et al.* used citric acid and urea to produce CDs with fluorescent patterning capabilities.[70] They also showed that their CDs had no observable toxicity in bean sprouts and mice.[70] As a testament to their low toxicity, they applied their CDs on human skin and showed their use as a low-toxicity method of obtaining fingerprints.[70] Interestingly, CDs can exhibit excellent stability in printed patterns and can retain their fluorescent properties for up to 3 months.[11] However, in high-security applications, it is important that this fluorescence remains stable for several years. Therefore, more work is required to study and extend the long-term stability of green-synthesized CDs.

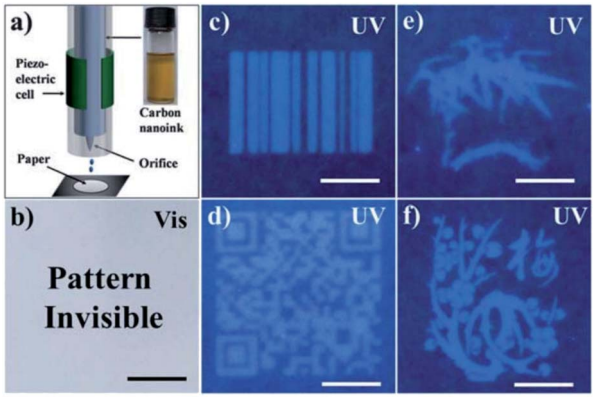


Fig. 5 (a) Inkjet printing using CDs synthesized from oriental plane leaves. (b) Invisible pattern made from CD ink under visible light. (c–f) Fluorescent patterns made from CD ink under UV light. Scale bar = 1 cm. Reproduced from RSC ref. 68. Copyright 2013 The Royal Society of Chemistry.

### 4.5 Catalysis

With their high surface area-to-volume ratio and their versatile functional groups, CDs find application in catalysis. CDs synthesized from willow bark were used as a photocatalyst for the fabrication of a Au nanoparticle/reduced graphene oxide nanocomposite, demonstrating that the CDs effectively reduced both materials.[12] The resulting nanocomposite was used in a system that catalyzes the reaction of glucose and oxygen into $H_2O_2$ allowing it to be an indirect method of glucose sensing *via* the detection of $H_2O_2$.[12] In another study, Essner *et al.* synthesized CDs from citric acid.[71] They first used their CDs to reduce $HAuCl_4$ to Au nanoparticle/CD hybrids at room temperature.[71] They also showed that the CDs can reduce $AgNO_3$ to Ag nanoparticle/CD hybrids, albeit at elevated temperatures and with NaOH.[71] They further demonstrated the performance of this Ag nanoparticle/CD hybrid as a catalyst to reduce 4-nitrophenol into 4-aminophenol in the presence of $NaBH_4$.[71] The use of waste products in green synthesis is often desirable to reduce the overall environmental impact of the synthesis process. For instance, Shih *et al.* synthesized CDs from used coffee grounds.[72] The resulting CDs were used to synthesize $Cu_{2-x}S$/CD hybrid nanomaterials which were integrated into a modified rotating disk electrode with a higher oxygen reduction reaction activity than its commercial Pt/C-modified counterpart.[72] These studies highlight the diverse catalytic applications of CDs, particularly towards the synthesis of novel hybrid nanomaterials.

## 5. Conclusions and outlook

We have established what constitutes a green CD synthesis by considering some of the 12 Principles of Green Chemistry regarding the use of non-hazardous renewable materials, safe synthesis methods, and where possible, lowered energy

requirements.[13] The green synthesis of CDs is mainly performed using hydrothermal (or solvothermal), microwave, and dry heating methods. Plants are the most common feedstock for CD synthesis, although renewable refined compounds such as citric acid and amino acids have also been used. Purification of CDs is typically done using a combination of filtration, centrifugation, and/or dialysis.

Despite considerable advances in the green CD literature, several challenges need to be addressed to improve their range of application. Demand for sensors with increasing sensitivity requires the exploration of novel green CD detection platforms that go beyond the traditional approach of CD–analyte interactions. For instance, a third intermediary compound can often be used in conjunction with a CD to measure the concentration of an analyte that the CD or intermediary alone may fail to detect. In the field of bioimaging, the need for a wide variety of fluorescence wavelengths requires further research into the green synthesis of CDs with higher peak excitation/emission wavelengths. Moreover, while sensing and bioimaging are the most examined applications of green-synthesized CDs, their potential in other applications, such as catalysis and optoelectronics, remains largely untapped.

CDs are a diverse category of nanomaterials with endless production pathways. Closing the knowledge gap between CDs produced from green synthesis methods and those manufactured by traditional methods requires a deeper understanding of the relationship between the CD precursor, the synthesis and purification methods employed, the resulting CD's physicochemical properties, and the effect of these parameters on the performance of the CDs in various applications. The establishment of correlations between the physical (*e.g.*, size, shape) and chemical (*e.g.*, N : C, O : C) properties of a CD and the resulting optical properties (*e.g.*, peak excitation/emission wavelength, QY) and performance towards various applications will be essential to advance the field.

## Conflicts of interest

There are no conflicts to declare.

## Acknowledgements

The authors acknowledge funding from the Natural Sciences and Engineering Research Council of Canada, Canada Research Chairs Program, Killam Research Fellowship, Fonds de recherche du Québec – Nature et technologies and the Quebec Center for Advanced Materials. S. Chahal acknowledges NSERC for a PGS D scholarship, McGill University for a MEDA, and the EUL fund in the Department of Chemical Engineering. J.-R. Macairan is grateful for a FAS fellowship from Concordia University.

## References

1 X. Xu, R. Ray, Y. Gu, H. J. Ploehn, L. Gearheart, K. Raker and W. A. Scrivens, *J. Am. Chem. Soc.*, 2004, **126**, 12736–12737.
2 H. Li, S. Ye, J. Guo, H. Wang, W. Yan, J. Song and J. Qu, *Nano Res.*, 2019, **12**, 3075–3084.
3 S.-T. Yang, X. Wang, H. Wang, F. Lu, P. G. Luo, L. Cao, M. J. Meziani, J.-H. Liu, Y. Liu, M. Chen, Y. Huang and Y.-P. Sun, *J. Phys. Chem. C*, 2009, **113**, 18110–18114.
4 W. S. Hummers and R. E. Offeman, *J. Am. Chem. Soc.*, 1958, **80**, 1339.
5 Q. Wang, H. Zheng, Y. Long, L. Zhang, M. Gao and W. Bai, *Carbon*, 2011, **49**, 3134–3140.
6 X. Jiang, D. Qin, G. Mo, J. Feng, C. Yu, W. Mo and B. Deng, *J. Pharm. Biomed. Anal.*, 2019, **164**, 514–519.
7 S. Chahal, N. Yousefi and N. Tufenkji, *ACS Sustainable Chem. Eng.*, 2020, **8**, 5566–5575.
8 A. Kumar, A. R. Chowdhuri, D. Laha, T. K. Mahto, P. Karmakar and S. K. Sahu, *Sens. Actuators, B*, 2017, **242**, 679–686.
9 Y. Wan, M. Wang, K. Zhang, Q. Fu, M. Gao, L. Wang, Z. Xia and D. Gao, *Microchem. J.*, 2019, **148**, 385–396.
10 M. Shahshahanipour, B. Rezaei, A. A. Ensafi and Z. Etemadifar, *Mater. Sci. Eng., C*, 2019, **98**, 826–833.
11 S. Bhatt, M. Bhatt, A. Kumar, G. Vyas, T. Gajaria and P. Paul, *Colloids Surf., B*, 2018, **167**, 126–133.
12 X. Qin, W. Lu, A. M. Asiri, A. O. Al-Youbi and X. Sun, *Catal. Sci. Technol.*, 2013, **3**, 1027–1035.
13 P. T. Anastas and J. C. Warner, *Green Chemistry: Theory and Practice*, Oxford University Press, New York, 1998.
14 E. Arkan, A. Barati, M. Rahmanpanah, L. Hosseinzadeh, S. Moradi and M. Hajialyani, *Adv. Pharm. Bull.*, 2018, **8**, 149–155.
15 L. Liu, Z. Mi, Q. Hu, C. Li, X. Li and F. Feng, *Anal. Methods*, 2019, **11**, 353–358.
16 D. Gu, S. Shang, Q. Yu and J. Shen, *Appl. Surf. Sci.*, 2016, **390**, 38–42.
17 R. Bao, Z. Chen, Z. Zhao, X. Sun, J. Zhang, L. Hou and C. Yuan, *Nanomater*, 2018, **8**, 386.
18 P. K. Yadav, V. K. Singh, S. Chandra, D. Bano, V. Kumar, M. Talat and S. H. Hasan, *Adv. Pharm. Bull.*, 2019, **5**, 623–632.
19 J. Shi, G. Ni, J. Tu, X. Jin and J. Peng, *J. Nanopart. Res.*, 2017, **19**, 209.
20 W. Liu, H. Diao, H. Chang, H. Wang, T. Li and W. Wei, *Sens. Actuators, B*, 2017, **241**, 190–198.
21 Z. Zhang, B. Hu, Q. Zhuang, Y. Wang, X. Luo, Y. Xie and D. Zhou, *Anal. Lett.*, 2020, **53**, 1704–1718.
22 H. Huang, J.-J. Lv, D.-L. Zhou, N. Bao, Y. Xu, A.-J. Wang and J.-J. Feng, *RSC Adv.*, 2013, **3**, 21691–21696.
23 W. Lu, X. Qin, S. Liu, G. Chang, Y. Zhang, Y. Luo, A. M. Asiri, A. O. Al-Youbi and X. Sun, *Anal. Chem.*, 2012, **84**, 5351–5357.
24 P. Zuo, J. Liu, H. Guo, C. Wang, H. Liu, Z. Zhang and Q. Liu, *Anal. Bioanal. Chem.*, 2019, **411**, 1647–1657.
25 Z. Zhang, J. Chen, Y. Duan, W. Liu, D. Li, Z. Yan and K. Yang, *Lumin*, 2018, **33**, 318–325.
26 D. Bano, V. Kumar, V. K. Singh and S. H. Hasan, *New J. Chem.*, 2018, **42**, 5814–5821.
27 Z. Wei, B. Wang, Y. Liu, Z. Liu, H. Zhang, S. Zhang, J. Chang and S. Lu, *New J. Chem.*, 2019, **43**, 718–723.
28 M. Wang, Y. Wan, K. Zhang, Q. Fu, L. Wang, J. Zeng, Z. Xia and D. Gao, *Anal. Bioanal. Chem.*, 2019, **411**, 2715–2727.

29 J. Zhou, Z. Sheng, H. Han, M. Zou and C. Li, *Mater. Lett.*, 2012, **66**, 222–224.
30 M. Xue, Z. Zhan, M. Zou, L. Zhang and S. Zhao, *New J. Chem.*, 2016, **40**, 1698–1703.
31 X. Yang, D. Wang, N. Luo, M. Feng, X. Peng and X. Liao, *Spectrochim. Acta, Part A*, 2020, **239**, 118462.
32 N. Murugan and A. K. Sundramoorthy, *New J. Chem.*, 2018, **42**, 13297–13307.
33 Q. Huang, Q. Li, Y. Chen, L. Tong, X. Lin, J. Zhu and Q. Tong, *Sens. Actuators, B*, 2018, **276**, 82–88.
34 R. Sobhani, B. Rezaei, M. Shahshahanipour, A. A. Ensafi and G. Mohammadnezhad, *Anal. Bioanal. Chem.*, 2019, **411**, 3115–3124.
35 N. Amin, A. Afkhami, L. Hosseinzadeh and T. Madrakian, *Anal. Chim. Acta*, 2018, **1030**, 183–193.
36 B. Rooj, A. Dutta, S. Islam and U. Mandal, *J. Fluoresc.*, 2018, **28**, 1261–1267.
37 W. A. Lotfy, K. M. Ghanem and E. R. El-Helow, *Bioresour. Technol.*, 2007, **98**, 3470–3477.
38 K. L. Penniston, S. Y. Nakada, R. P. Holmes and D. G. Assimos, *Journal of Endourology*, 2008, **22**, 567–570.
39 Y. Qu, L. Yu, B. Zhu, F. Chai and Z. Su, *New J. Chem.*, 2020, **44**, 1500–1507.
40 F. Noun, J. Manioudakis and R. Naccache, *Part. Part. Syst. Charact.*, 2020, **37**, 2000119.
41 J. B. Essner, J. A. Kist, L. Polo-Parada and G. A. Baker, *Chem. Mater.*, 2018, **30**, 1878–1887.
42 M. L. Liu, B. B. Chen, C. M. Li and C. Z. Huang, *Green Chem.*, 2019, **21**, 449–471.
43 N. Vasimalai, V. Vilas-Boas, J. Gallo, M. d. F. Cerqueira, M. Menéndez-Miranda, J. M. Costa-Fernández, L. Diéguez, B. Espiña and M. T. Fernández-Argüelles, *Beilstein J. Nanotechnol.*, 2018, **9**, 530–544.
44 S. Chandra, D. Laha, A. Pramanik, A. Ray Chowdhuri, P. Karmakar and S. K. Sahu, *Lumin*, 2016, **31**, 81–87.
45 G. Wu, M. Feng and H. Zhan, *RSC Adv.*, 2015, **5**, 44636–44641.
46 Q. Wang, X. Huang, Y. Long, X. Wang, H. Zhang, R. Zhu, L. Liang, P. Teng and H. Zheng, *Carbon*, 2013, **59**, 192–199.
47 R. F. Domingos, M. A. Baalousha, Y. Ju-Nam, M. M. Reid, N. Tufenkji, J. R. Lead, G. G. Leppard and K. J. Wilkinson, *Environ. Sci. Technol.*, 2009, **43**, 7277–7284.
48 Q.-C. Sun, Y. C. Ding, D. M. Sagar and P. Nagpal, *Prog. Surf. Sci.*, 2017, **92**, 281–316.
49 Q. Liang, W. Ma, Y. Shi, Z. Li and X. Yang, *Carbon*, 2013, **60**, 421–428.
50 A. T. R. Williams, S. A. Winfield and J. N. Miller, *Anal*, 1983, **108**, 1067–1071.
51 Y. Zhang, X. Liu, Y. Fan, X. Guo, L. Zhou, Y. Lv and J. Lin, *Nanoscale*, 2016, **8**, 15281–15287.
52 J. Liao, Z. Cheng and L. Zhou, *ACS Sustainable Chem. Eng.*, 2016, **4**, 3053–3061.
53 W. Chen, L. Yan and P. R. Bangal, *Carbon*, 2010, **48**, 1146–1152.
54 K. Radhakrishnan and P. Panneerselvam, *RSC Adv.*, 2018, **8**, 30455–30467.
55 N. Murugan, M. Prakash, M. Jayakumar, A. Sundaramurthy and A. K. Sundramoorthy, *Appl. Surf. Sci.*, 2019, **476**, 468–480.
56 N. Pourreza and M. Ghomi, *Mater. Sci. Eng., C*, 2019, **98**, 887–896.
57 S. Konar, B. N. P. Kumar, M. K. Mahto, D. Samanta, M. A. S. Shaik, M. Shaw, M. Mandal and A. Pathak, *Sens. Actuators, B*, 2019, **286**, 77–85.
58 B. Rezaei, Z. Hassani, M. Shahshahanipour, A. A. Ensafi and G. Mohammadnezhad, *Lumin*, 2018, **33**, 1377–1386.
59 L. Wang, Y. Bi, J. Hou, H. Li, Y. Xu, B. Wang, H. Ding and L. Ding, *Talanta*, 2016, **160**, 268–275.
60 A. A. Ensafi, S. H. Sefat, N. Kazemifard and B. Rezaei, *J. Iran. Chem. Soc.*, 2019, **16**, 355–363.
61 A. A. Ensafi, S. Hghighat Sefat, N. Kazemifard, B. Rezaei and F. Moradi, *Sens. Actuators, B*, 2017, **253**, 451–460.
62 H. M. Ahmed, M. Ghali, W. K. Zahra and M. Ayad, *Mater. Today: Proc.*, 2020, **33**, 1845–1848.
63 Z. Lai, X. Guo, Z. Cheng, G. Ruan and F. Du, *ChemistrySelect*, 2020, **5**, 1956–1960.
64 Z. Ramezani, M. Qorbanpour and N. Rahbar, *Colloids Surf., A*, 2018, **549**, 58–66.
65 X. Wei, L. Li, J. Liu, L. Yu, H. Li, F. Cheng, X. Yi, J. He and B. Li, *ACS Appl. Mater. Interfaces*, 2019, **11**, 9832–9840.
66 K. Dehvari, K. Y. Liu, P.-J. Tseng, G. Gedda, W. M. Girma and J.-Y. Chang, *J. Taiwan Inst. Chem. Eng.*, 2019, **95**, 495–503.
67 Y. Shao, C. Zhu, Z. Fu, K. Lin, Y. Wang, Y. Chang, L. Han, H. Yu and F. Tian, *J. Nanopart. Res.*, 2020, **22**, 229.
68 L. Zhu, Y. Yin, C.-F. Wang and S. Chen, *J. Mater. Chem. C*, 2013, **1**, 4925–4932.
69 J. Wang, F. Peng, Y. Lu, Y. Zhong, S. Wang, M. Xu, X. Ji, Y. Su, L. Liao and Y. He, *Adv. Opt. Mater.*, 2015, **3**, 103–111.
70 S. Qu, X. Wang, Q. Lu, X. Liu and L. Wang, *Angew. Chem., Int. Ed.*, 2012, **51**, 12215–12218.
71 J. B. Essner, C. H. Laber and G. A. Baker, *J. Mater. Chem. A*, 2015, **3**, 16354–16360.
72 Z.-Y. Shih, A. P. Periasamy, P.-C. Hsu and H.-T. Chang, *Appl. Catal., B*, 2013, **132–133**, 363–369.